EurJOC
European Journal of Organic Chemistry

Full Papers
doi.org/10.1002/ejoc.202001644

Chemistry Europe
European Chemical Societies Publishing

Arsenic-Bridged Silafluorene and Germafluorene as a Novel Class of Mixed-Heteroatom-Bridged Heterofluorenes

Hiroshi Sasaki,[a] Ippei Akioka,[a] Hiroaki Imoto,*[a, b] and Kensuke Naka*[a, b]

Arsenic-bridged silafluorene and germafluorene were synthesized as a novel class of mixed-heteroatom-bridged heterofluorenes. Their structures, photophysical properties, and electronic natures were studied by experimental and computational means. The doubly-bridged biphenyl moieties were distorted from the reported singly-bridged ones. The intersystem crossing from the singlet excitation states to the triplet ones was enhanced by the arsenic-bridging structures, implying that bridging through an arsenic atom is favorable for phosphorescence.

Introduction

The fusion of heteroatoms into π-conjugated systems is an important tool to attain the unique structure, reactivity, and optoelectronic properties. Heterofluorene, heteroatom-bridged biphenyl, is one of the most typical frameworks to incorporate heteroatoms into π-conjugation. The resultant heterofluorene materials reflect the intrinsic nature of the elements. The elements employed for heterofluorene have been expanding to heavy atoms such as gallium,[1] germanium,[2] arsenic,[3] *etc.* There are systematic studies on a series of heterofluorenes, which cover a variety of elements.[4] For example, Kuehne synthesized a series of heterofluorene-based polymers to reveal that the photophysical properties such as emission wavelength, quantum yield, and amplified spontaneous emission are highly dependent on the fused elements.[4g]

For further electronic perturbation, heteroatom-bridged heterofluorene, which has a second heteroatom, has recently attracted considerable attention. As a pioneering work, Shimizu and Hiyama reported that silicon-bridged silafluorene attains expansion of the σ*-π* conjugation as well as adopts a highly planar conformation.[5] Moreover, Yamaguchi showed that phosphoryl-bridged phosphafluorene oxide can enhance the electron-acceptance when compared with the conventional phosphafluorene oxide.[6] On the other hand, mixed-heteroatom-bridged heterofluorenes, which contain two kinds of bridging elements, have been rarely examined so far; sulfur-bridged silafluorene is a limited example.[7] A computational study of C,N-, C,Si-, and N,S-bridged fluorenes was conducted in 2020.[8]

We have been working on the development of functional organoarsenic chemistry, particularly π-conjugated materials.[9] In a series of arsole derivatives, arsafluorenes can show phosphorescence, though phosphafluorenes exhibit only fluorescence.[3a] It is rational that bridging the heterofluorenes by an arsenic atom should be beneficial for phosphorescence due to the heavy-atom effect as well as the enhanced rigidity (Figure 1). In this work, we selected silafluorene and germafluorene as the target heterofluorenes bridged by an arsenic atom because they are suitable for demonstration for the effects of the bridging arsenic atoms due to sufficient stability. Additionally, no stereoisomers are not produced after bridging by an arsenic atom because of the C_{2v}-symmetrical structures of 9,9-dimethyl-silafluorene and 9,9-dimethylgermafluorene, and thus the synthetic procedures would be simple. Herein, arsenic-bridged dimethylsilafluorene and dimethylgermafluorene were synthesized, and their structures and optoelectronic properties were investigated in comparison to those of 9-phenylarsafluorene,[3a] 9,9-dimethylsilafluorene,[11] 9,9-dimethylgermafluorene.[12] The bridging structures affected the emission behaviors. This is the first study on arsenic-bridged heterofluorenes.

[a] *H. Sasaki, I. Akioka, Prof. Dr. H. Imoto, Prof. Dr. K. Naka*
Faculty of Molecular Chemistry and Engineering,
Graduate School of Science and Technology
Kyoto Institute of Technology
Goshokaido-cho, Matsugasaki, Sakyo-ku,
Kyoto 606-8585, Japan
E-mail: himoto@kit.ac.jp
kenaka@kit.ac.jp
http://www.cis.kit.ac.jp/~kenaka/index_eng.html
[b] *Prof. Dr. H. Imoto, Prof. Dr. K. Naka*
Materials Innovation Lab,
Kyoto Institute of Technology,
Goshokaido-cho, Matsugasaki, Sakyo-ku, Kyoto 606-8585, Japan

Supporting information for this article is available on the WWW under https://doi.org/10.1002/ejoc.202001644

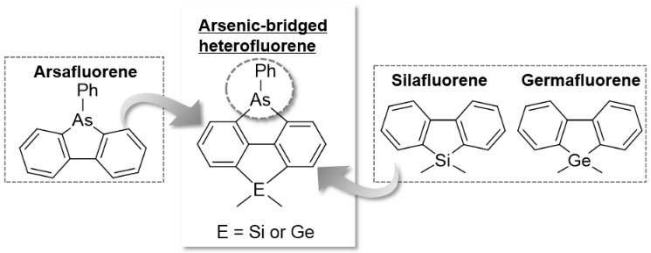

Figure 1. Molecular design of the arsenic-bridged heterofluorenes, *i.e.*, silafluorene and germafluorene, investigated in the present work.

Results and Discussion

Dimethylsilyl- and dimethylgermyl-bridged 9-phenylarsafluorenes (**3a** and **3b**, respectively) were synthesized as shown in Scheme 1. 2,2′,6,6′-Tetrabromobiphenyl (**1**)[13] was di-lithiated by *n*-butyllithium (*n*-BuLi), and diiodophenylarsine ($PhAsI_2$)[3a] was added to obtain 4,5-dibromo-9-phenyl-arsafluorene (**2**). After di-lithiation of **2**, addition of dichlorodimethylsilane (Me_2SiCl_2) or dichlorodimethylgermane (Me_2GeCl_2) produced arsenic-bridged heterofluorenes **3a** and **3b**, respectively. The chemical structures of **2**, **3a**, and **3b** were determined by NMR, high-resolution mass analysis, and single-crystal X-ray diffraction (XRD) analysis.[14] The solids and solutions of **3a** and **3b** were stable under ambient conditions for at least several months.

The single crystals of **3a** and **3b** suitable for XRD were grown by recrystallization from dichloromethane and methanol (Figure 2). For comparison, the structure of 9,9-dimethylgermafluorene (**5b**) were analyzed (for detail, see supporting information) and those of 9-phenyarsafluorene (**4**)[3a] and 9,9-dimethylsilafluorene (**5a**)[15] was cited from the previous papers. Both the singly and doubly-bridged biphenyls adopted highly planar structures. The C–C single bond of the biphenyl moieties

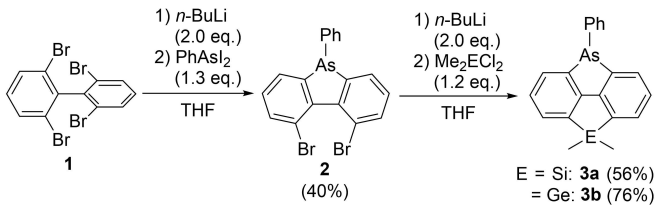

Scheme 1. Synthesis of arsenic-bridged heterofluorenes **3a** and **3b**.

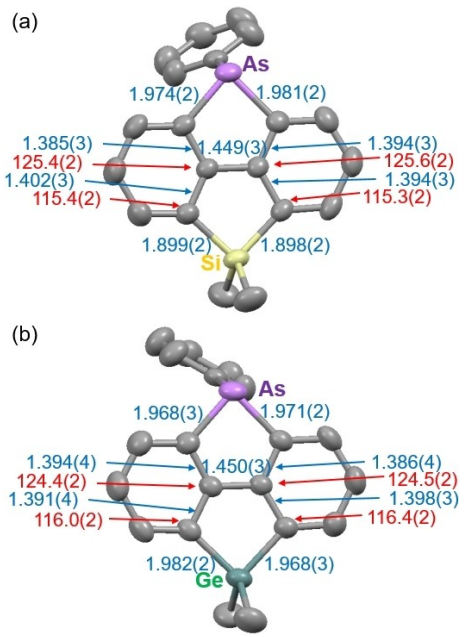

Figure 2. ORTEP and selected bond lengths (Å, blue) and angles (°, red) of (a) **3a** and (b) **3b**. Hydrogen atoms are omitted for clarity. Thermal ellipsoids are drawn at the 50% probability level.

was shortened by the bridging through the silane and germane; the C–C bond lengths were 1.449(3) Å (**3a**), 1.450(3) Å (**3b**), 1.479(6) Å (**4**), 1.488(5) and 1.495(5) Å (**5a**), and 1.49(1) and 1.50(1) Å (**5b**). Considering the internal angles, the fused benzene rings of **3** were distorted from those of non-bridged heterofluorenes **4** and **5**. That is, the distributions of the inner angles of **3a** and **3b** (**3a**: 115.3(2)–125.6(2)°, **3b**: 116.0(2)–124.5(2)°) were wider than those of **4**, **5a**, and **5b** (**4**: 119.3(4)–121.2(5)°, **5a**: 118.4(3)–121.5(3)°, **5b**: 118.4(6)–122.0(7)°). These results suggested that the doubly-bridged biphenyl moieties of **3a** and **3b** were strained when compared with the singly-bridged ones of **4**, **5a**, and **5b**. In addition, the phenyl groups on the arsenic atoms of **3a** and **3b** were tilted to one of the phenylene rings, when compared with the optimized structures (*vide infra*). This is probably because of the molecular packing.

The aromaticity of the heterole rings of **3–5** was estimated by nucleus-independent chemical shift (NICS) value and bond alternation (Figure 3).[16] The geometries were fully optimized by density functional theory (DFT) calculations based on B3LYP/6-31G+(d,p).[17] The $NICS(1)_{zz}$ values, which were obtained by GIAO–B3LYP/6-311G+(d,p), were 4.3 (arsole of **3a**), 7.0 (silole of **3a**), 4.8 (arsole of **3b**), 6.6 (germole of **3b**), 2.9 (**4**), 9.4 (**5a**), and 7.6 (**5b**). Considering that the calculated $NICS(1)_{zz}$ value of benzene was −29.1, the heterole rings of **3–5** were non-aromatic. We estimated the Wiberg bond indices (WBIs) of the heterole rings in **3–5** by conducting natural bond orbital (NBO) analysis using DFT calculations at the B3LYP/6-31G(d) level of theory.[18] The WBIs of **3–5** indicated that the heteroles have bond-alternations, corresponding to the X-ray observations (Figure 2). Thus the heteroles of **3–5** were lack of conjugation, which well agreed with the results of the NICS estimations.

The photophysical properties of **3a** and **3b** were examined in comparison with those of **4**, **5a**, and **5b** as summarized in Table 1. The UV-vis absorption spectra were measured in 2-methyltetrahydrofuran (2-MeTHF) solutions ($c = 1.0 \times 10^{-5}$ mol/L) (Figure 4a). The longest absorption maxima (λ_{abs}) of **3a** (285 nm) and **3b** (284 nm) were similar to singly-bridged heterofluorenes (λ_{abs} = 279 nm (**4**), 277 nm (**5a**), 277 nm (**5b**)). DFT and time-dependent DFT (TD-DFT) calculations was

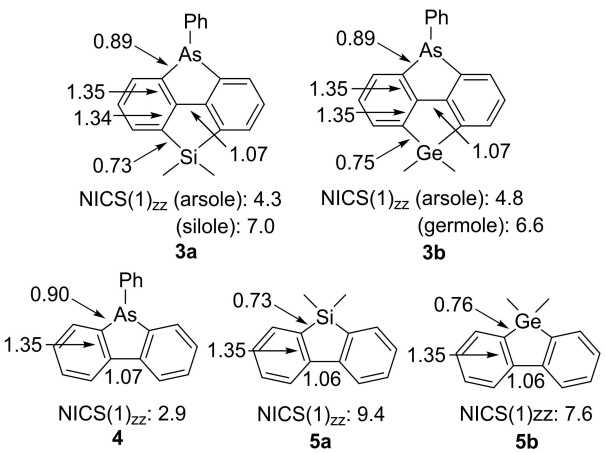

Figure 3. $NICS(1)_{zz}$ values and WBIs of the heteroles of **3–5**.

Table 1. Optical properties of **3–5**.

	298 K					77 K			
	Solution (2-MeTHF)[a]			Solid		Solution (2-MeTHF)[a]		Solid	
	λ_{abs}[b] [nm]	λ_{ex}[c] [nm]	λ_{em}[d] [nm] (Φ[e])	λ_{ex}[c] [nm]	λ_{em}[d] [nm] (Φ[e])	λ_{ex}[c] [nm]	λ_{em}[d] [nm] (Φ[e])	λ_{ex}[c] [nm]	λ_{em}[d] [nm] (Φ[e])
3a	285	308	341 (<0.01)	n.d.	n.d.	297	359 (<0.01) 490 (<0.01)	348	401 (0.01) 543 (0.13)
3b	284	278	332 (<0.01)	n.d.	n.d.	295	354 (<0.01) 489 (<0.01)	342	393 (0.02) 539 (0.29)
4	279	280	307 (<0.01)	n.d.	n.d.	293	345 (<0.01) 489 (<0.01)	322	399 (<0.01) 524 (<0.01)
5a	277	276	341 (0.24)	257	350 (0.34)	278	333 (0.33) 486 (<0.01)	255	343 (0.41)
5b	277	285	332 (<0.01)	259	341 (<0.01)	291	338 (<0.01) 490 (<0.01)	265	355 (<0.01)

[a] $c = 1.0 \times 10^{-5}$ mol/L. [b] Absorption maxima. [c] Excitation maxima. [d] Emission maxima. [e] Absolute quantum yields.

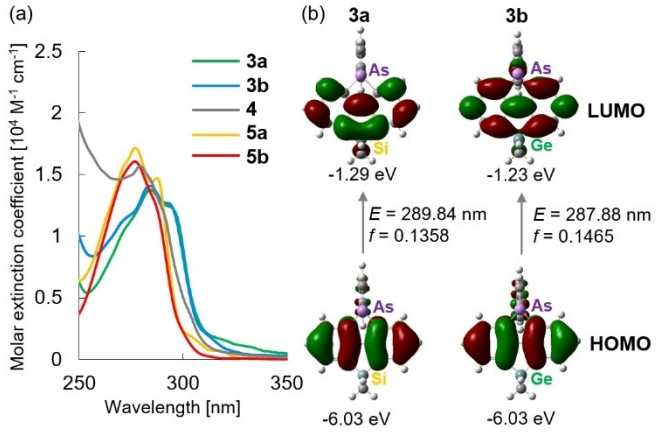

Figure 4. (a) UV-vis absorption spectra of **3–5** ($c = 1.0 \times 10^{-5}$ mol/L in 2-MeTHF), and (b) frontier orbitals of **3a** and **3b**: HOMO and LUMO levels, and transition energies (*E*) and oscillator strengths (*f*) for the HOMO-LUMO transitions.

conducted to understand the electron transitions for the absorption (B3LYP/6-31G + (d,p)) (Figure 4b). The fully optimized structures were used for the calculations. The TD-DFT calculations revealed that the highest occupied molecular orbitals (HOMOs) and lowest unoccupied molecular orbitals (LUMOs) were responsible for the absorption considering the oscillator strengths (*f*). The estimated transition energies (*E*) were similar, and it is thus evident that the absorption wavelengths of **3–5** were similar. The HOMOs of **3–5** were located at the biphenyl moieties, and the LUMOs included σ*-π* conjugations besides the biphenyl moieties. The σ*-π* conjugation for the LUMO of **3a** was contributed by the σ* orbital of the C–Si bond, whereas that of **3b** was due to the C–As bond. This means that the conjugations of **3a** and **3b** were not expanded to the whole of the doubly-bridged biphenyls, resulting in similar UV-vis absorption spectra to those of singly-bridged biphenyls **4**, **5a**, and **5b**.

The photoluminescence (PL) spectra of **3–5** were then measured in the solution ($c = 1.0 \times 10^{-5}$ M in 2-MeTHF) and solid states. Initially, the measurements were carried out at room temperature. In solutions, luminescence was observed around 300–400 nm for all the compounds (Figure 5a). The emission maxima (λ_{em}) were similar for **3–5** (307–341 nm), corresponding to the absorption spectra. The quantum yield (Φ) of **5a** (Φ = 0.24) was remarkably higher than the others. In the solid states (Figure 5b), **3a**, **3b**, and **4** showed negligible emission, though **5a** and **5b** emitted the fluorescence at the similar wavelengths to those in the solutions: **5a** (λ_{em} = 350 nm) and **5b** (λ_{em} = 341 nm). When measured in solutions at 77 K (Figure 5c), the longer-wavelength emissions appeared in the range of 420–600 nm in addition to the shorter-wavelength emissions for all the compounds. On the other hand, in the solid states (Figure 5d), **5a** and **5b** showed fluorescence, whereas the longer-wavelength emissions were dominant in **3a**, **3b**, and **4**. The λ_{em}s of **3a**, **3b**, and **4** were red-sifted in the solid states from the solutions because of the intermolecular interactions. The emission lifetimes for the shorter-wavelength emissions of **4**, **5a**, and **5b** were measured in the solid-state at 77 K to be on the ns order, suggesting that they are attributed to fluorescence. On the other hand, the emissions of **3a** and **3b** and the longer-wavelengths emissions of **4**, **5a**, and **5b** were too weak under any conditions to measure the lifetimes. However, it is rational that the longer-wavelength emissions are attributed to phosphorescence.

For further understanding of the emission properties of **3–5**, the energy levels at the S_n and T_n (n = 1, 2, 3…) states were analyzed by TD-DFT calculations at B3LYP/ for C, H, and SDD for Si, Ge, As (Figure S16). The full geometries were optimized at the S_1 states. It is notable that there were multiple low-lying T_n states under the S_1 states for **3–5** (**3a**, **4**, **5b**: T_1-T_3, **3b**: T_1–T_4, **5a**: T_1 and T_2). Therefore, the intersystem crossing (ISC) for all the compounds was likely to occur. On the other hand, Si atom is less beneficial for ISC than As and Ge atoms from the viewpoint of heavy-atom effect. This is why the fluorescence was dominant in **5a** under all the conditions. In turn, the emissions of **3a**, **3b**, **4**, and **5b** were quite weak at room temperature in the solution and solid states. It is probable that the ISC effectively occurred, and the excitons at the T_n states were deactivated *via* non-radiative thermal motions at room temper-

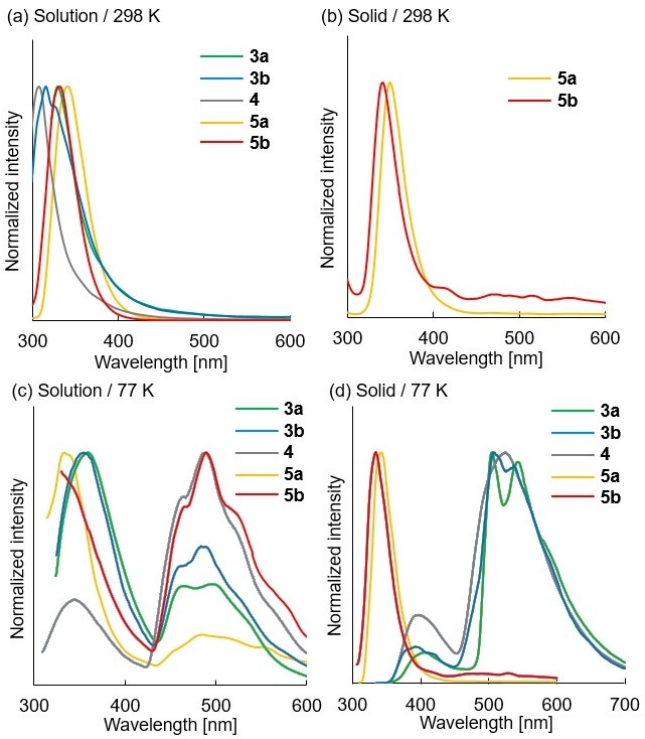

Figure 5. PL spectra of **3–5**: (a) solution ($c = 1.0 \times 10^{-5}$ mol/L in 2-MeTHF) and (b) solid at 298 K, and (c) solution ($c = 1.0 \times 10^{-5}$ mol/L in 2-MeTHF) and (d) solid at 77 K. The emissions of **3a**, **3b**, and **4** in the solid states at 298 K were too weak, and the spectra were omitted from (b) for clarity.

ature. The phosphorescence was observed when the molecular motions were frozen states at 77 K. In particular, the emission efficiency for the phosphorescence of **3a** and **3b** was significantly high, and the Φ of **3b** (0.29) was higher than that of **3a** (0.13). This result means that the doubly-bridged structures using the arsenic atom, being a heavy atom, were effective to freeze the molecular motions and that the heavy-atom effect of the Ge atom enhanced the ISC.

Conclusion

In the present work, arsenic-bridged silafluorene and germafluorene were synthesized as a novel class of mixed-heteroatom-bridged heterofluorenes. The obtained dimethylsilyl- and dimethylgermyl-bridged 9-phenylarsafluorenes (**3a** and **3b**, respectively) are the first examples of arsenic-bridged heterofluorenes. The doubly-bridged biphenyl moieties of **3a** were strained when compared with the singly-bridged ones of **4**, **5a**, and **5b**. On the other hand, the heterole rings of **3–5** were non-aromatic, regardless of the bridging fashion. The bridging arsenic atoms could effectively promote the ISC from the singlet excitation states to the triplet ones when compared with Si and Ge, considering the results of the photophysical studies at 77 K. We are now extensively investigating the effect of the arsenic atom on phosphorescence as well as the development of other arsenic-bridged heterofluorenes, and the results will be reported in future publications.

Experimental Section

Materials

Chloroform ($CHCl_3$), dichloromethane (CH_2Cl_2), methanol (MeOH), sodium thiosulfate pentahydrate ($Na_2S_2O_3 \cdot 5H_2O$), copper(II) chloride anhydrous ($CuCl_2$), and dimethyldichlorosilane (Me_2SiCl_2) were purchased from Nacalai Tesque, Inc (Kyoto, Japan). Tetrahydrofuran (THF), diethyl ether (Et_2O), *n*-hexane, *n*-buthyllitium (*n*-BuLi, 1.6 M in hexane solution), iodine (I_2), magnesium sulfate ($MgSO_4$), sodium chloride (NaCl), and distilled water were purchased from Wako Pure Chemical Industry, Ltd (Osaka, Japan). Dimethyldichlorogermane (Me_2GeCl_2), lithium diisopropylamide (LDA, *ca.* 20% in THF/Ethylbenzene/Heptane, *ca.* 1.5 mol/L), and 2-methyltetrahydrofuran (2-MeTHF) were purchased from Sigma-Aldrich Co., Ltd. 1,2-Dibromobenzene and 1,3-dibromobenzene were purchased from Tokyo Chemical Industry Co., Ltd (Tokyo, Japan). All commercially available chemicals were used without further purification. 2,2′-Dibromobiphenyl,[19] 2,2′,6,6′-tetrabromobiphenyl (**1**)[12] and 9-phenyl-9-arsafluorene (**4**),[3a] and hexaphenylhexaarsine (As_6Ph_6)[20] were prepared according to literature procedures.

Measurement

^1H (400 MHz), ^{13}C (100 MHz), and ^{29}Si (80 MHz) nuclear magnetic resonance (NMR) spectra were recorded on a Bruker AVANCE III 400 NMR spectrometer. High-resolution mass spectra (HRMS) were obtained on a JEOL JMS-SX102 A spectrometer. UV/Vis spectra were recorded on a JASCO spectrophotometer V-670 KNN. Emission and excitation spectra were obtained on an FP-8500 (JASCO) spectrometer and the absolute PL quantum yields (Φ) were determined by using a JASCO ILFC-847S; the quantum yield of quinine sulfate as a reference was 0.52, which is in agreement with the literature value.[21] Emission lifetimes were measured by using a Quantaurus-Tau (Hamamatsu Photonics, Shizuoka, Japan) instrument.

X-ray crystallographic data for single-crystalline products

The single crystal was mounted on a glass fiber. Intensity data were collected at room temperature on a Rigaku XtaLAB mini with graphite monochromated Mo Kα radiation. Readout was performed in the 0.073 mm pixel mode. The data were collected to a maximum 2θ value of 55.0°. Data were processed using the Crystal Clear program[22] and CrysAlisPro.[23] An analytical numeric absorption correction[24] was applied. The data were corrected for Lorentz and polarization effects. The structure was solved by the direct method[25] and ShelXT[26] and expanded using Fourier techniques. Non-hydrogen atoms were refined anisotropically. Hydrogen atoms were refined using the riding model. The final cycle of full-matrix least-squares refinement on F^2 was based on observed reflections and variable parameters. All calculations were performed using the CrystalStructure[27] or Olex2[28] crystallographic software package except for refinement, which was performed using SHELXL2013,[29] SHELXL2016[30] respectively.

Synthesis

Note: Low molecular weight organoarsenic compounds have volatility, and it is necessary to avoid the procedures generating volatile organoarsenic compounds. For safety, experiments should

be performed in a fume hood. Besides, in a few cases, spontaneously flammable compounds are obtained as described in the literature,[31] and thus fire prevention measures should be taken.

4,5-Dibromo-9-phenyl-9-arsafluorene (2). To a THF solution (25.0 mL) of **1** (1.01 g, 2.15 mmol) was added *n*-BuLi (1.6 M in *n*-hexane, 2.70 mL, 4.32 mmol) at −78 °C under N_2 atmosphere. After stirring at −78 °C for 2 h, a THF solution (2.0 mL) of $PhAsI_2$ (1.3 eq), which was prepared from As_6Ph_6 (427.3 g, 0.468 mmol) and I_2 (717.0 g, 2.83 mmol),[3a] was added dropwise to the reaction mixture. The resulting mixture was gradually warmed to room temperature and stirred for 14 h. Distilled water was poured into the reaction mixture at 0 °C, and the organic layer was concentrated *in vacuo*. The aqueous layer was extracted with CH_2Cl_2, and the combined organic layer was dried over $MgSO_4$. After filtration, the solvents were removed *in vacuo*. The residue was purified through the silica column chromatography (eluent: *n*-hexane). The title compound was obtained as light yellow solids (398 mg, 0.86 mmol, 40%). A single crystal of **2** was obtained by recrystallization (CH_2Cl_2/MeOH). ^{1}H-NMR (acetone-d_6, 400 MHz): δ 7.84 (dd, J = 7.2, 1.2 Hz, 2H), 7.75 (dd, J = 7.2, 1.2 Hz, 2H), 7.44–7.38 (t, J = 7.4 Hz, 2H), 7.29–7.21 (m, 5H) ppm; ^{13}C-NMR (acetone-d_6, 100 MHz): δ 148.8, 144.9, 140.0, 134.8, 131.8, 130.0, 129.7, 129.1, 129.0, 119.9 ppm; HR-FAB-MS (m/z): calculated for $C_{18}H_{12}Br_2As$ $[M+H]^+$, 460.8522; found, 460.8517.

4,8-Dihydro-4,4-dimethyl-8-phenylarsindoro[4,3,2-bcd]benzosilole (3a). To a THF solution (25.0 mL) of **2** (506.3 mg, 1.10 mmol) was added *n*-BuLi (1.6 M in *n*-hexane, 1.4 mL, 2.24 mmol) at −78 °C under N_2 atmosphere. After stirring at −78 °C for 2 h, a THF solution (2.0 mL) of Me_2SiCl_2 (0.16 mL, 1.32 mmol) was added dropwise to the reaction mixture. The resulting mixture was gradually warmed to room temperature, and stirred for 15 h. Distilled water was poured into the reaction mixture at 0 °C, and the organic layer was concentrated *in vacuo*. The aqueous layer was extracted with CH_2Cl_2, and the combined organic layer was dried over $MgSO_4$. After filtration, the solvents were removed *in vacuo*. The residue was purified through the silica column chromatography (eluent: *n*-hexane/ toluene = 100/1). The title compound was obtained as colorless solids (220 mg, 0.61 mmol, 56%). A single crystal of **3a** was obtained by recrystallization (CH_2Cl_2/MeOH). ^{1}H-NMR (acetone-d_6, 400 MHz): δ 7.79 (dd, J = 7.4, 0.8 Hz, 2H), 7.69 (dd, J = 7.4, 0.8 Hz, 2H), 7.44–7.38 (m, 2H), 7.31 (t, J = 7.4 Hz, 2H), 7.27–7.22 (m, 3H), 0.52 (s, 3H), 0.51 (s, 3H) ppm; ^{13}C-NMR ($CDCl_3$, 100 MHz): δ 158.5, 140.9, 139.5, 135.2, 132.4, 132.0, 128.7, 128.4, 128.1, −2.2, −2.4 ppm; ^{29}Si-NMR (acetone-d_6, 80 MHz): δ 13.1 ppm; HR-FAB-MS (m/z): calculated for $C_{20}H_{17}SiAs$ $[M]^+$, 360.0315; found, 360.0308.

4,8-Dihydro-4,4-dimethyl-8-phenylarsindoro[4,3,2-bcd] benzogermole (3b). To a THF solution (12.5 mL) of **2** (250.4 mg, 0.54 mmol) was added *n*-BuLi (1.6 M in *n*-hexane, 0.90 mL, 1.44 mmol) at −78 °C under N_2 atmosphere. After stirring at −78 °C for 2 h, a THF solution (1.0 mL) of Me_2GeCl_2 (0.08 mL, 0.69 mmol) was added dropwise to the reaction mixture. The resulting mixture was gradually warmed to room temperature, and stirred for 15 h. Distilled water was poured into the reaction mixture at 0 °C, and the organic layer was concentrated *in vacuo*. The aqueous layer was extracted with CH_2Cl_2, and the combined organic layer was dried over $MgSO_4$. After filtration, the solvents were removed *in vacuo*. The residue was purified through the silica column chromatography (eluent: *n*-hexane/ toluene = 100/1). The title compound was obtained as colorless solids (167 mg, 0.41 mmol, 76%). A single crystal of **3b** was obtained by recrystallization (CH_2Cl_2/MeOH). ^{1}H-NMR (acetone-d_6, 400 MHz): δ 7.77 (dd, J = 7.4, 0.8 Hz, 2H), 7.69 (dd, J = 7.4, 0.8 Hz, 2H), 7.44–7.38 (m, 2H), 7.32 (t, J = 7.4 Hz, 2H), 7.26–7.22 (m, 3H), 0.70 (s, 3H), 0.69 (s, 3H) ppm; ^{13}C-NMR ($CDCl_3$, 100 MHz): δ 157.5, 141.4, 139.7, 137.6, 132.4, 132.1, 131.4, 128.7, 128.4, 128.3, −1.2, −1.3 ppm; HR-FAB-MS (m/z): calculated for $C_{20}H_{17}GeAs$ $[M]^+$, 405.9758; found, 405.9768.

9,9-Dimethylsilafluorene (5a). To a THF solution (15.0 mL) of 2,2′-dibromobiphenyl (1.25 g, 4.00 mmol) was added *n*-BuLi (1.6 M in *n*-hexane, 5.0 mL, 8.0 mmol) at −78 °C under N_2 atmosphere. After stirring at −78 °C for 2 h, Me_2SiCl_2 (0.58 mL, 4.8 mmol) was added dropwise to the reaction mixture. The resulting mixture was gradually warmed to room temperature and stirred for 2 h. Distilled water was poured into the reaction mixture at 0 °C, and the organic layer was concentrated *in vacuo*. The aqueous layer was extracted with CH_2Cl_2, and the combined organic layer was dried over $MgSO_4$. After filtration, the solvents were removed *in vacuo*. The residue was purified through the silica column chromatography (eluent: *n*-hexane). The title compound was obtained as colorless solids (626 mg, 2.98 mmol, 74%). ^{1}H-NMR (acetone-d_6, 400 MHz): δ 7.90 (d, J = 8.0 Hz, 2H), 7.70 (d, J = 8.0 Hz, 2H), 7.43 (t, J = 7.6 Hz, 2H), 7.28 (t, J = 7.3 Hz, 2H), 0.41 (s, 6H) ppm; ^{13}C-NMR ($CDCl_3$, 100 MHz): δ 147.8, 139.0, 132.8, 130.2, 127.4, 120.8, −3.21 ppm; ^{29}Si-NMR ($CDCl_3$, 80 MHz): δ 0.39 ppm. These NMR data correspond to the reported ones.[10]

9,9-Dimethylgermafluorene (5b). To a THF solution (15.0 mL) of 2,2′-dibromobiphenyl (505 mg, 1.62 mmol) was added *n*-BuLi (1.6 M in *n*-hexane, 2.1 mL, 3.36 mmol) at −78 °C under N_2 atmosphere. After stirring at −78 °C for 2 h, a THF solution (1.0 mL) of Me_2GeCl_2 (0.20 mL, 1.73 mmol) was added dropwise to the reaction mixture. The resulting mixture was gradually warmed to room temperature and stirred for 2 h. Distilled water was poured into the reaction mixture at 0 °C, and the organic layer was concentrated *in vacuo*. The aqueous layer was extracted with CH_2Cl_2, and the combined organic layer was dried over $MgSO_4$. After filtration, the solvents were removed *in vacuo*. The residue was purified through the silica column chromatography (eluent: *n*-hexane). The title compound was obtained as colorless solids (333 mg, 1.31 mmol, 81%). A single crystal of **3b** was obtained by slow evaporation of saturated solution in MeOH. ^{1}H-NMR (acetone-d_6, 400 MHz): δ 7.90 (d, J = 8.0 Hz, 2H), 7.70 (d, J = 7.2 Hz, 2H), 7.41 (t, J = 7.6 Hz, 2H), 7.28 (t, J = 7.2 Hz, 2H), 0.57 (s, 6H) ppm; ^{13}C-NMR ($CDCl_3$, 100 MHz): δ 146.4, 141.2, 132.9, 129.5, 127.5, 121.4, −2.6 ppm. These NMR data correspond to the reported ones.[11]

Acknowledgements

This work was supported by JSPS KAKENHI, grant Number 19H04577 (Coordination Asymmetry) and 20H02812 (Grant-in-Aid for Scientific Research (B)) to HI.

Conflict of Interest

The authors declare no conflict of interest.

Keywords: Arsenic · Germanium · Heterofluorene · Phosphorescence · Silicon

[1] a) A. Decken, F. P. Gabbaï, A. H. Cowley, *Inorg. Chem.* **1995**, *34*, 15, 3853; b) T. Matsumoto, K. Tanaka, Y. Chujo, *J. Am. Chem. Soc.* **2013**, *135*, 4211; c) T. Matsumoto, K. Tanaka, Y. Chujo, *Macromolecules* **2015**, *48*, 1343; d) T. Matsumoto, H. Takamine, K. Tanaka, Y. Chujo, *Chem. Lett.* **2015**, *44*, 1658; e) T. Matsumoto, S. Ito, K. Tanaka, Y. Chujo, *Polym. J.* **2018**, *50*, 197.

[2] For recent papers, see: a) O. Shynkaruk, G. He, R. McDonald, M. J. Ferguson, E. Rivard, *Chem. Eur. J.* **2016**, *22*, 248; b) D. W. Hammerstroem, J. B. Wilking, N. P. Rath, *J. Organomet. Chem.* **2017**, *830*, 196; c) X.-Y. Liu, Q.-S. Tian, D. Zhao, Q. Ran, L.-S. Liao, J. Fan, *J. Mater. Chem. C* **2018**, *6*, 8144; d) T. G. Sedinkin, A. C. Herath, R. West, J. Y. Becker, *ChemElectroChem* **2019**, *6*, 4252.
[3] For recent papers: a) T. Kato, S. Tanaka, K. Naka, *Chem. Lett.* **2015**, *44*, 1476; b) H. Imoto, S. Tanaka, T. Kato, S. Watase, K. Matsukawa, T. Yumura, K. Naka, *Organometallics* **2016**, *35*, 364; c) H. Imoto, S. Tanaka, T. Kato, T. Yumura, S. Watase, K. Matsukawa, K. Naka, *Organometallics* **2016**, *35*, 3647; d) A. K. Gupta, S. Akkarasamiyo, A. Orthaber, *Inorg. Chem.* **2017**, *56*, 4504; e) H. Imoto, H. Sasaki, S. Tanaka, T. Yumura, K. Naka, *Organometallics* **2017**, *36*, 2605; f) H. Sasaki, H. Imoto, T. Kitao, T. Uemura, T. Yumura, K. Naka, *Chem. Commun.* **2019**, *55*, 6487; g) M. Olaru, D. Duvinage, Y. Naß, L. A. Malaspina, S. Mebs, J. Beckmann, *Angew. Chem. Int. Ed.* **2020**, *59*, 14414.
[4] For example, see: a) R.-F. Chen, Q.-L. Fan, C. Zheng, W. Huang, *Org. Lett.* **2006**, *8*, 203; b) K. Geramita, J. McBee, T. D. Tilley, *J. Org. Chem.* **2009**, *74*, 820; c) S. Zhang, R. Chen, J. Yin, F. Liu, H. Jiang, N. Shi, Z. An, C. Ma, B. Liu, W. Huang, *Org. Lett.* **2010**, *12*, 3438; d) J. Yin, S.-L. Zhang, R.-F. Chen, Q.-D. Ling, W. Huang, *Phys. Chem. Chem. Phys.* **2010**, *12*, 15448; e) T. Shimasaki, Y. Takiyama, Y. Nishihara, A. Morimoto, N. Teramoto, M. Shibata, *Tetrahedron Lett.* **2015**, *56*, 260; f) Z. Yu, Y.-S. Wu, J. Chen, C. Sun, H. Fu, *Phys. Chem. Chem. Phys.* **2016**, *18*, 32678; g) V. H. K. Fell, A. Mikosch, A.-K. Steppert, W. Ogieglo, E. Senol, D. Canneson, M. Bayer, F. Schoenebeck, A. Greilich, A. J. C. Kuehne, *Macromolecules* **2017**, *50*, 2338.
[5] M. Shimizu, H. Tatsumi, K. Mochida, K. Oda, T. Hiyama, *Chem. Asian J.* **2008**, *3*, 1238.
[6] a) E. Yamaguchi, A. Studer, S. Yamaguchi, *Angew. Chem. Int. Ed.* **2011**, *50*, 12094; b) T. W. Greulich, N. Suzuki, C. G. Daniliuc, A. Fukazawa, E. Yamaguchi, A. Studer, S. Yamaguchi, *Chem. Commun.* **2016**, *52*, 2374; c) T. W. Greulich, E. Yamaguchi, C. Doerenkamp, M. Lebbesmeyer, C. G. Daniliuc, A. Fukazawa, H. Eckert, S. Yamaguchi, A. Studer, *Chem. Eur. J.* **2017**, *23*, 6029.
[7] T. Kimura, Y. Izumi, N. Furukawa, Y. Minoshima, *Heteroat. Chem.* **1996**, *7*, 143.
[8] Y. Qi, C. Chen, C. Zheng, Y. Tang, Y. Wan, H. Jiang, T. Chen, Y. Tao, R. Chen, *Phys. Chem. Chem. Phys.* **2020**, *22*, 3675.
[9] For reviews, see: a) H. Imoto, *Polym. J.* **2018**, *50*, 837; b) H. Imoto, K. Naka, *Chem. Eur. J.* **2019**, *25*, 1883.
[10] T. Ureshino, T. Yoshida, Y. Kuninobu, K. Takai, *J. Am. Chem. Soc.* **2010**, *132*, 14324.
[11] M. Tobisu, K. Baba, N. Chatani, *Org. Lett.* **2011**, *13*, 3282.
[12] S. M. Kilyanek, X. Fang, R. F. Jordan, *Organometallics* **2009**, *28*, 300.
[13] Deposition Numbers 2051372 (**2**), 2051371 (**3a**), 2051370 (**3b**), and 2051373 (**5b**) contain the supplementary crystallographic data for this paper. These data are provided free of charge by the joint Cambridge Crystallographic Data Centre and Fachinformationszentrum Karlsruhe Access Structures service www.ccdc.cam.ac.uk/structures.
[14] K. Ishijima, S. Tanaka, H. Imoto, K. Naka, *Dalton Trans.* **2020**, *49*, 15612.
[15] J. Mewes, H.-W. Lerner, M. Bolte, *Acta Crystallogr.* **2009**, *E65*, o451.
[16] a) Z. Chen, C. S. Wannere, C. Corminboeuf, R. Puchta, P. von R. Schleyer, *Chem. Rev.* **2005**, *105*, 3842; b) H. F.-B. Shaidaei, C. S. Wannere, C. Corminboeuf, R. Puchta, P. von R. Schleyer, *Org. Lett.* **2006**, *8*, 863.
[17] Gaussian 16, Revision C.01, M. J. Frisch, G. W. Trucks, H. B. Schlegel, G. E. Scuseria, M. A. Robb, J. R. Cheeseman, G. Scalmani, V. Barone, G. A. Petersson, H. Nakatsuji, X. Li, M. Caricato, A. V. Marenich, J. Bloino, B. G. Janesko, R. Gomperts, B. Mennucci, H. P. Hratchian, J. V. Ortiz, A. F. Izmaylov, J. L. Sonnenberg, D. Williams-Young, F. Ding, F. Lipparini, F. Egidi, J. Goings, B. Peng, A. Petrone, T. Henderson, D. Ranasinghe, V. G. Zakrzewski, J. Gao, N. Rega, G. Zheng, W. Liang, M. Hada, M. Ehara, K. Toyota, R. Fukuda, J. Hasegawa, M. Ishida, T. Nakajima, Y. Honda, O. Kitao, H. Nakai, T. Vreven, K. Throssell, J. A. Montgomery, Jr., J. E. Peralta, F. Ogliaro, M. J. Bearpark, J. J. Heyd, E. N. Brothers, K. N. Kudin, V. N. Staroverov, T. A. Keith, R. Kobayashi, J. Normand, K. Raghavachari, A. P. Rendell, J. C. Burant, S. S. Iyengar, J. Tomasi, M. Cossi, J. M. Millam, M. Klene, C. Adamo, R. Cammi, J. W. Ochterski, R. L. Martin, K. Morokuma, O. Farkas, J. B. Foresman, D. J. Fox, Gaussian, Inc., Wallingford CT, 2016.
[18] A. E. Reed, L. A. Curtiss, F. Weinhold, *Chem. Rev.* **1988**, *88*, 899.
[19] A. A. Ageshina, G. K. Sterligov, S. A. Rzhevskiy, M. A. Topchiy, G. A. Chesnokov, P. S. Gribanov, E. K. Melnikova, M. S. Nechaev, A. F. Asachenko, M. V. Bermeshev, *Dalton Trans.* **2019**, *48*, 3447.
[20] J. W. B. Reesor, G. F. Wright, *J. Org. Chem.* **1957**, *22*, 382.
[21] K. Kinoshita, K. Mihashi, *Fluorescence Measurements, Application to Bioscience, Measurement Method, Series 3;* Spectroscopical Society of Japan, Academic Publication Center.
[22] *CrystalClear: Data Collection and Processing Software*, Rigaku Corporation (1998– β014). Tokyo 196–8666, Japan.
[23] *CrysAlisPro: Data Collection and Processing Software*, Rigaku Oxford Diffraction, **2020**, Tokyo 196–8666, Japan.
[24] Analytical numeric absorption correction using a multifaceted crystal model. R. C. Clark, J. S. Reid, *Acta Crystallogr.* **1995**, *A51*, 887.
[25] *SHELXS2013*: G. M. Sheldrick, *Acta Crystallogr.* **2008**, *A64*, 112.
[26] *SHELXT*: G. M. Sheldrick, *Acta Crystallogr.*, **2015**, *C71*, 3.
[27] *CrystalStructure 4.1*: *Crystal Structure Analysis Package*, Rigaku Corporation (β000–β014). Tokyo 196–8666, Japan.
[28] *Olex2*: O. V. Dolomanov, L. J. Bourhis, R. J. Gildea, J. A. K. Howard, H. Puschmann, *J. Appl. Crystallogr.* **2009**, 42, 339.
[29] *SHELXL2013*: G. M. Sheldrick, *Acta Crystallogr. Sect. A* **2008**, 64, 11β.
[30] *SHELXL2016*: G. M. Sheldrick, *Acta Crystallogr.* **2015**, *C27*, 3.
[31] I. Fleming Ed., *Science of Synthesis Category 1, vol 4*; G. Thieme: Stuttgart, Germany 2002; Chapter 4.1, pp 13.

Manuscript received: December 20, 2020
Revised manuscript received: January 24, 2021
Accepted manuscript online: January 27, 2021